

# Interstellar Iron and Silicon Depletions in Translucent Sight Lines<sup>1</sup>

Adam Miller<sup>2,3</sup> and J. T. Lauroesch<sup>4</sup>

*Department of Physics and Astronomy, Northwestern University, 2145 Sheridan Road,  
Evanston, IL 60208*

amiller@ast.cam.ac.uk, jtl@elvis.astro.northwestern.edu

Ulysses J. Sofia

*Department of Astronomy, Whitman College, 345 Boyer Avenue, Walla Walla, WA 99362*

sofiauj@whitman.edu

Stefan I. B. Cartledge<sup>5</sup>

*Department of Physics and Astronomy, Louisiana State University, Baton Rouge, LA  
70803*

scartled@gmail.com

and

David M. Meyer

*Department of Physics and Astronomy, Northwestern University, 2145 Sheridan Road,  
Evanston, IL 60208*

davemeyer@northwestern.edu

## ABSTRACT

We report interstellar Fe II and Si II column densities toward six translucent sight lines ( $A_V \gtrsim 1$ ) observed with the Space Telescope Imaging Spectrograph (STIS). The abundances were determined from the absorption of Si II] at 2335 Å, and several weak Fe transitions including the first reported detections of the 2234 Å line. We derive an empirical  $f$ -value for the Fe II  $\lambda 2234$  Å transition of  $\log(f\lambda) = -1.54 \pm 0.05$ . The observed sight lines sample a variety of extinction characteristics as indicated by their  $R_V$  values, which range from 2.6 - 5.8. The dust-phase abundances of both Si and Fe are positively correlated with the small-grain population (effective radii smaller than a few hundred  $\mu\text{m}$ ) toward

the targets. The physical conditions along the sight lines suggest that this relationship may be due to differences in the survival of small particles in some interstellar environments. The chemical composition of the small grains could either resemble dust mantles or be silicate rich.

*Subject headings:* dust – ISM: abundances

## 1. Introduction

Highly abundant species play a significant role in the formation of interstellar dust grains, and thus are important to our understanding of the chemical evolution of interstellar clouds. Interstellar silicon and iron abundances are two of the most important diagnostics for studying dust. Only oxygen and carbon make up a higher fraction of grain mass, and the large abundances and volatility of these elements make it difficult to determine their precise dust-phase abundances. Conversely, silicon and iron can provide us with detailed information about the dust composition in sight lines that sample a wide range of physical conditions. Silicates appear to be ubiquitous in the neutral ISM (Vladilo 2002; Sofia et al. 2006), and iron always shows a substantial depletion from the gas phase (Jenkins 1987). Thus silicon and iron are fundamental grain constituents of most interstellar dust models (Draine 2003).

The dominant ions of iron and silicon in the neutral ISM are Fe II and Si II. Previous surveys of interstellar Fe II and Si II abundances were performed with data from *Copernicus* (Jenkins, Savage & Spitzer 1986) and the *International Ultraviolet Explorer (IUE)* (van Steenberg & Shull 1988) satellites. These measurements suffered from the limitations (particularly background uncertainties and limited spectral resolution) of both instruments,

---

<sup>1</sup>Based on observations with the NASA/ESA *Hubble Space Telescope*, obtained from the data archive at the Space Telescope Science Institute. STScI is operated by the Association of Universities for Research in Astronomy, Inc. under NASA contract NAS 5-26555.

<sup>2</sup>Visiting student from the Massachusetts Institute of Technology (MIT).

<sup>3</sup>Current Address: Institute of Astronomy, University of Cambridge, Madingley Road, Cambridge. CB3 0HA, UK.

<sup>4</sup>Current Address: Department of Physics and Astronomy, University of Louisville, Louisville, KY 40292.

<sup>5</sup>Current Address: Department of Physics & Astronomy, Valparaiso University, 1610 Campus Drive East, Valparaiso, IN 46383

and to a lesser degree from large uncertainties associated with the  $f$ -values for the absorption lines used in these studies. This situation was greatly improved with the launch of the *Hubble Space Telescope (HST)*, which has superior spectral resolution and sensitivity. Such data can be used to detect the extremely weak lines that are unlikely to suffer from saturation effects.

In the past decade, new accurate laboratory  $f$ -values have been determined for numerous transitions of important species including the Fe II  $\lambda\lambda 2249, 2260$  Å lines (Bergeson, Mullman & Lawler 1994) as well as the very weak inter-system Si II]  $\lambda 2335$  Å line (Calami, Smith & Bergeson 1993). Despite these improvements, very few reliable measurements of both the iron and silicon abundance in the same sight line have been made. Additionally, as we begin to look at higher column density sight lines even the (relatively) weak Fe II transitions at  $\lambda\lambda 1142, 2249, 2260$  Å, which have well known oscillator strengths, begin to suffer from saturation effects. Therefore, even weaker lines such as the Fe II transitions at  $\lambda 2234$  and  $2367$  Å are important for an accurate determination of column densities. Unfortunately the Fe II transitions at  $\lambda 2234$  and  $2367$  Å do not have experimentally derived  $f$ -values.

In this paper we use these very weak iron and silicon lines to investigate the translucent sight line abundances. The goal is to better understand the dust characteristics of these sight lines, which have previously been extensively studied for carbon, oxygen, and krypton abundances (Cartledge et al. 2001; Sofia et al. 2004). In §2 we discuss the sample and the data. In §3 we present the iron and silicon depletions, and discuss the results in §4.

## 2. Observations and Data Reduction

The six primary sight lines for this study were originally selected for determining the abundance of interstellar carbon (Sofia et al. 2004). A summary of the sight line characteristics for our sample is given in Table 1. As discussed by Sofia et al. (2004), the weakness of the interstellar  $2325$  Å C II] feature required very high signal-to-noise ratios to be obtained with the E230H echelle mode of STIS aboard the *Hubble Space Telescope*. Within the wavelength region covered by these observations are also located the weak intersystem line of Si II] at  $2335$  Å and multiple transitions of Fe II including the very weak absorption lines at  $2234$  Å and  $2367$  Å. A detailed description of the data is given in Sofia et al. (2004). As discussed in that paper, a number of tests were performed with these datasets to obtain the most reliable measurements of weak lines. In addition to the *HST* spectra, *Far-Ultraviolet Spectroscopic Explorer (FUSE)* data from Cartledge et al. (2004) were used. Figure 1 shows the normalized Si (*solid line*) and Fe (*dotted line*) absorption features for each of the sight lines superimposed on different vertical scales.

### 3. Results

#### 3.1. Ionization and Excited States

Based on the ionization potentials of neutral iron and silicon (7.9 and 8.1 eV respectively), it is natural to assume that the dominant state contributing to the iron and silicon columns in the H I gas in our six lines of sight would be the ground-state of Fe II and Si II, which have ionization potentials of 16.2 and 16.3 eV respectively. In deriving the gas-phase abundances of these elements one also has to consider the low-lying excited-states of Si II and Fe II which can be populated by collisions and/or photon pumping, in addition to the neutral and doubly-ionized states. We note that besides the ground-state transitions of Si II and Fe II, transitions arising from Si I and Fe I and the excited states of Si II and Fe II are within our wavelength coverage or within the wavelength coverage of the E140H ( $\lambda_{cent} = 1271 \text{ \AA}$ ) data obtained for these stars discussed in Cartledge et al. (2001). While the Si III (1206Å) line is covered, its intrinsic strength makes it an unsuitable transition for determination of the column density of doubly-ionized silicon. Therefore we will use measurements of the populations of neutral and singly-ionized silicon and iron as well as evidence from other elements to determine if the assumption that the ground state of singly-ionized iron and silicon indeed dominate the columns in the H I gas is correct.

We can derive the neutral columns from the Fe I (2167, 2198Å) and Si I (2208Å) lines in our datasets. These lines are generally very weak, indeed the largest equivalent width for Fe I (2167Å) is detected toward HD 147888 at  $15.7 \pm 0.9 \text{ m\AA}$ , corresponding to a column density of  $3 \times 10^{12} \text{ cm}^{-2}$ , or  $\sim 0.1\%$  of the Fe II column. Even toward HD 27778, with the lowest column of Fe II in our sample, the neutral fraction is less than 1%. For Si I the line at 2208.67 Å has an oscillator strength of  $5.75 \times 10^{-2}$  (Morton 2003), a factor of  $1.35 \times 10^4$  times larger than the Si II] (2335Å) line. Since the equivalent widths of this Si I line are at most five times that of the Si II] line toward any star, we see that neutral silicon is  $< 0.1\%$  of the total silicon in these sight lines.

The excited states of Fe II and Si II can be populated by either collisions (with H I and/or electrons) and/or by photon pumping by ultraviolet photons (Bahcall & Wolf 1968). For only two of the six sight lines studied do we see significant absorption due to the excited state transitions of either Si II or Fe II: toward the stars HD 37021 and HD 37061. Since there are lines arising in multiple excited states of Fe II in our STIS E230H datasets we first measured the column densities or upper limits for states of Fe II with excitation potentials up to  $3117.5 \text{ cm}^{-1}$  (0.39 eV) toward both HD 37021 and HD 37061. We note that toward HD 37061 we detect absorption for states up to the  $1872.6 \text{ cm}^{-1}$  (0.24 eV) level, while toward HD 37021 only the  $1872.6 \text{ cm}^{-1}$  level has detectable absorption. Such lines have

been observed previously in a range of contexts: e.g., circumstellar disks (Lagrange et al. 1996), ejecta from  $\eta$  Carina (Gull et al. 2005), and circumstellar outflow from the progenitor of SN 1998S (Bowen et al. 2000). We derived total column densities for the sum of all of these states of  $\sim 5 \times 10^{12} \text{ cm}^{-2}$  and  $\sim 2 \times 10^{13} \text{ cm}^{-2}$  for HD 37021 (summed over both components, see below) and HD 37061, respectively, which imply that  $<1\%$  of the Fe II column is in these excited states toward both stars.

The situation for Si II in these two sight lines is more complicated – the non-detection of the 2335.321 Å line of Si II\* (the  $287.2 \text{ cm}^{-1}$  (0.036 eV) level) in our E230H datasets does not place a significant constraint on the column density, the limits are  $\sim 64\%$  and  $\sim 35\%$  of the Si II column for HD 37021 and HD 37061, respectively. The lines in the E140H datasets for these stars are also not useful as all five lines of Si II\* between 1194 and 1309 Å are highly saturated. Since we cannot directly measure the column density of Si II\*, we turn to models using the excitation of Fe II and C II to estimate the contribution of Si II\* to  $N(\text{Si II})$ .

First we considered the HD 37061 sight line where we can use the columns of the Fe II  $3d^6(^5D)4s\ a^6D$  levels as well as the columns of C II and C II\* from Sofia et al. (2004) to derive an electron density which can be used to estimate the Si II\* in this absorption component. For Fe II we used the two lowest energy states (0.385 and 0.667 eV) of the  $3d^6(^5D)4s\ a^6D$  level, where we detected four lines for each state, and derived column densities of  $1.7 \pm 0.1 \times 10^{12} \text{ cm}^{-2}$  and  $0.6 \pm 0.2 \times 10^{12} \text{ cm}^{-2}$  respectively. For C II we used the ratio of the excited to the ground-state ( $N(\text{C II}^*)/N(\text{C II}) \sim 0.5$ ) measured by Sofia et al. (2004). Using the measured column density ratios and the models of the excitation of C II and Si II from Smeding & Pottasch (1979) and of Fe II from Keenan et al. (1988), we see that for temperatures of  $\sim 1\text{--}3,000 \text{ K}$  (consistent with the inferred b-value)  $N(\text{Si II}^*)/N(\text{Si II}) \lesssim 10\%$  for this sight line. At these temperatures the excitation of C II suggests that  $n_{\text{H}} \sim 10^3 \text{ cm}^{-3}$  and  $n_{\text{e}} \sim 10 \text{ cm}^{-3}$ , implying that hydrogen is  $\sim 1\%$  ionized in this component.

The excitation equilibrium arguments given above for HD 37061 suggest the Si II and Fe II absorption detected in these weak lines corresponds to the bulk of the H I along this sight line, and does not include a large component associated with an H II region(s). A similar argument holds for the other sight lines, and further evidence of the lack of a large H II region contribution to these columns is the generally good agreement between the observed C II, O I, and Kr I columns in these sight lines and the local interstellar mean values. Except for HD 152590, the sight lines show no evidence for significant enhancements of the C II column suggestive of potential H II region contamination (Sofia et al. 2004). For HD 152590 the column density of C II (and perhaps Kr I) is significantly larger than the mean value, this sight line is the only sight line in our sample at large distances (Cartledge et al. 2001; Sofia et al. 2004).

### 3.2. Column Densities

We measured the equivalent widths or upper limits of the Fe II  $\lambda\lambda$  2234, 2249, 2260, 2344, 2367, 2374, 2382 Å transitions in our *HST* data, as well as the Si II]  $\lambda$  2335 Å intersystem transition (see Figure 1). For four of these stars (all but HD 37021 and 37061) we used *FUSE* data to measure the equivalent widths of the Fe II  $\lambda\lambda$  1055, 1142, 1143, and 1144 Å lines. With the exception of the 2234 and 2367 Å transitions, we adopted the oscillator strengths from Morton (2003) to derive curves-of-growth for each sight line. The equivalent width and the corresponding optically thin column density for each of the above lines toward HD 147888 are presented in Table 2, with the resulting curve-of-growth for HD 147888 shown in Figure 2. From this plot, it is clear that  $\lambda\lambda$ 1144, 2344, 2374, 2382 are all extremely optically thick lines, and that the Raasen & Uylings (1998)  $f$ -value for 2234 Å seems to underestimate the Fe II column density.

For the Fe II  $\lambda$ 2367 Å line there are several different  $f$ -values in the literature. The value given in Morton (2003) ( $\log f\lambda = -1.291$ ) is based upon theoretical calculations, while that given by Cardelli & Savage (1995) ( $\log f\lambda = -0.827$ ) was empirically derived from observations of several interstellar sight lines. Welty et al. (1999) suggested revising the Cardelli & Savage (1995) oscillator strength upwards to reflect revisions in the oscillator strengths of the other Fe II lines used by Cardelli & Savage (1995) to determine that value. We adopt the  $f$ -value from Welty et al. (1999) ( $\log f\lambda = -0.713$ ) for  $\lambda$ 2367 Å based on the curves-of-growth for the sight lines in this study. Were we to adopt the Morton (2003)  $f$ -value the measured equivalent widths of this line would imply that the Fe II columns toward HD 37021, HD37061, and HD 147888 should increase by factors of 0.53, 0.54, and 0.53 dex, respectively. Similarly, use of the Cardelli & Savage (1995) oscillator strength would imply an increase the Fe column densities for all three sight lines by 0.11 dex. For the stars HD 152590 and HD 207198 it appears that the profiles of the 2367 Å transition fail to fully reflect the multiple distinguished absorption components in these sight lines (Cartledge et al. 2001) based upon the Fe II 2249 Å transition. We note that the column densities, based on direct measurements of the Fe II 2249 Å transition for these sight lines may be underreported due to saturation. For HD 27778 we do not detect the Fe II 2367 Å transition at a statistically significant level, and therefore instead adopt the value derived from the apparent optical depth integral for the 2249 and 2260 Å transitions which is consistent with the column derived from the curve-of-growth. In addition, we have included the error due to uncertainties in the oscillator strengths in deriving the uncertainties in the resulting Fe II column densities based upon the curve-of-growth. Errors were taken from Morton (2003) for the STIS lines except 2367 Å where we have used the error estimate of Cardelli & Savage (1995), for the *FUSE* lines we have used the error estimates from Howk et al. (2000). We use the equivalent width of the Si II] 2335 Å line to directly derive the column density for Si II from the weak line limit.

The uncertainty in the equivalent widths take into account both photon noise (Jenkins et al. 1973) and the uncertainty in the continuum placement (Sembach, Savage & Massa 1991; Savage, Cardelli & Sofia 1992) added in quadrature. In Table 1 we list a representative Fe II transition used, the equivalent widths ( $W_\lambda$ ) for the listed Fe II line and Si II] 2335Å, and the respective column densities ( $N$ ) for our sight lines and  $\zeta$  Oph. We have also separately listed the errors in the Si II column density including the uncertainty in the oscillator strength from Morton (2003) added in quadrature – while not relevant for intercomparisons between sightlines using the same (weak) transition, such errors can be relevant for intercomparisons between sightlines using different absorption lines.

### 3.3. Fe II $\lambda$ 2234 Å Detection

The ( $^4F_{10}^0$ ) Fe II  $\lambda$ 2234 Å transition was detected toward three sight lines: HD 37021, HD 37061, and HD 147888. Each of these detections was at the  $4\sigma$  level or better. Figure 3 shows the normalized flux of the 2234 Å (*solid line*) absorption feature toward each of these targets. The normalized flux of the 2367 Å (*dotted line*) absorption feature has been superimposed over these data with a different vertical scale. The figure suggests that, while the 2234 Å feature is very weak, it is present and detectable along high column density sight lines.

The only available  $f$ -value for 2234 Å ( $\log f\lambda = -1.249$ ; Morton 2003) is based on the theoretical work of Raasen & Uylings (1998). Were we to adopt this oscillator strength the Fe II column densities for HD 37021, HD 37061, and HD 147888 would decrease by 0.15 dex, 0.37 dex, and 0.34 dex, respectively. By fitting the measured equivalent widths for 2234 Å to the curves of growth for HD 37021, HD 37061, and HD 147888, we have instead derived an empirical  $f$ -value of  $\log f\lambda = -1.54 \pm 0.05$  for this transition. For each sight line we first determined the column density and associated error using a curve-of-growth, we then calculated what the corresponding oscillator strength (as well as its error) would be given the observed equivalent width and error for the 2234 Å line. The derived oscillator strength was then determined by taking the weighted mean for each sight line based upon equivalent width measurement uncertainties. Our estimate of the uncertainty is the error in the weighted mean from these three determinations.

#### 4. Discussion

Although dust grains containing silicon and iron are common in the ISM, it is not clear what their size distributions or origins are (Zubko et al. 2004). Using a simplistic dust model, Sofia et al. (2005) find that sight lines with larger mass-fractions in small grains have a higher percentage of their silicon in the form of dust, and that the "extra" silicon is depleting primarily into small particles with effective radii  $< 200 \mu\text{m}$ . Although the model suggests that an additional population rather than grain processing is responsible for the enhanced small-grain populations, the authors warn that their result must be interpreted with caution. The model that they used was quite simple, so their results were meant to be merely suggestive.

The present data set represents the first sample of high-quality interstellar gas-phase Si and Fe measurements in sight lines exhibiting substantial levels of extinction and having measured  $c_4$  and  $R_V$  values (Valencic, Clayton, & Gordon 2004). Although our data only sample a small number of targets, these sight lines and measured abundances are ideal for exploring the small grain population. However, we must first convert gas-phase abundances to dust-phase abundances and/or depletions. Typically one adopts as the reference for the current total (dust + gas) abundances the Solar-system values, since the required set of cosmic abundance standards for current interstellar matter in and around the Solar-neighborhood is not currently established (Savage & Sembach 1996). We note that it does appear that the interstellar medium is well-mixed, since the variations between sight lines in the interstellar gas-phase abundances of elements such as O I and Kr I are small (see for example Cartledge et al. (2003, 2004)). Thus if the "true" interstellar reference abundances are different than the proto-sun reference abundances of Lodders (2003) used here, the differences will amount to just a uniform offset in the measured number of atoms in the dust-phase for silicon and iron for these sight lines.

One measure of the small grain population is the  $c_4$  variable in the Fitzpatrick & Massa (1988) extinction parameterization, which describes the strength of the extinction from 1050 to 1695 Å (Sofia et al. 2005). Specifically, Fitzpatrick & Massa (1988) found a polynomial common to extinction curves that fits  $E(\lambda - V)/E(B - V)$  as a function of wavenumber below 1695 Å. The  $c_4$  parameter is the amplitude of this extinction component for a given sight line. The polynomial is a continuously decreasing function from 1050 to 1695 Å, therefore larger  $c_4$  values correspond to steeper extinction curves over these wavelengths. Since extinction in this wavelength region is produced by small grains either composed of carbon (Mathis, Rumpl & Nordsieck 1977; Deśert et al. 1990) or silicates (Mathis 1996; Li & Draine 2001; Clayton et al. 2003),  $c_4$  can be used as a proxy for grain size distribution; larger  $c_4$  values correspond to a higher fraction of small grains along a sight line. The ratio



of total-to-selective extinction,  $R_V = A_V/E(B - V)$ , can also serve as a proxy for dust size distributions with smaller  $R_V$  values indicating a larger fraction of mass in small grains. In Figure 4 we display the silicon and iron dust-phase abundances as a function of sight line  $c_4$  values. The figure shows that in higher- $c_4$  sight lines a smaller fraction of Si and Fe atoms are in the gas phase, suggesting that sight lines with enhanced populations of small grains have more of these elements incorporated into dust. Using  $R_V$  as a proxy for dust-size distributions produces a similar result, however there is no correlation between depletions and  $E(B-V)$  in our sample. This suggests that the dust-phase abundance variations of Si and Fe are truly related to grain-size populations rather than to the strength of extinction. A linear fit to the Si data in Figure 4 (a higher order polynomial is not statistically justifiable) indicates that there is a 6% rise in the silicon dust-phase abundance per increase of 1.0 in  $c_4$ . Sofia et al. (2005) found that in order to fit the extinction in their sample, their model required 12% more silicon to be in dust per 1.0 increase in  $c_4$ . The quantitative difference in these results is likely due to the simplicity of the model used to fit the extinction.

There are two plausible, non-exclusive explanations for the correlation between depletions and  $c_4$  (or  $R_V$ ). The first is that the excess of elements depleted from the high- $c_4$  sight lines is incorporated into a new population of small grains; these grains would exist in addition to the grains found in lower- $c_4$  regions. Alternatively, a grain population that has been processed to a smaller average size could result in enhanced depletions. The increased surface-to-volume ratio would augment the number of surface sites available, and thus allow enhanced mantling.

Carbon appears to be under-abundant in the gas toward HD 27778 (Sofia et al. 2004), which also shows the most extreme Si and Fe depletions. The least-depleted sight lines in our sample, toward HD 37021 and HD 37061 (both in Orion), show low molecular fractions and significantly higher radiation fields. The physical characteristics of these sight lines suggest that the measured depletions may be due to differences in the survival of small grains in some interstellar environments, perhaps coupled with additional mantling onto grain surfaces. We note that Larson & Whittet (2005) also find that enhanced small grain populations (as indicated by low  $R_V$  values) are common in high-latitude translucent-cloud sight lines where one might expect relatively low radiation fields.

Figure 5 shows dust-phase silicon abundances plotted as a function of dust-phase Fe abundances for regions that sample a wide variety of neutral ISM environments, from halo clouds to the translucent sight lines of our sample. The solid line in the figure shows the weighted linear least squares fit to the data; the slope is 3.46 and the y-intercept is -80.42. Statistically this is a valid fit to the points, with 69% of the  $1\sigma$  error bars intersecting the line. We note, however, that those data points with dust-phase Fe values below 34 per million

H (PMH) could be better fit with a less-steep line (shown as a dashed line in Figure 5); a fit to the points with  $(\text{Fe}/\text{H})_{\text{dust}}$  greater than 34 PMH produces a line that is similar to the solid one plotted in the figure. Given the small number of points in Figure 5 and the large uncertainties of the data at smaller dust abundances, we cannot conclude with certainty whether a one or a two line fit is appropriate for the plotted data. We note that in neither case could the illustrated linear fits extend to indefinitely low values of dust abundances; both would have more than half of the iron in dust when silicon is entirely in the gas phase. At some point Fe has to deplete more efficiently from the gas than Si, which would result in a less steep relationship than that shown by the lines in Figure 4.

The one and two line fits to the Figure 5 data result in different interpretations for the small grain population. The single-line scenario suggests that over the large range of physical conditions sampled by the sight lines, Si and Fe are being depleted into dust in a ratio that is equal to the line’s slope, 3.46 Si atoms to every Fe atom. Further, if the differences in elemental dust–phase abundances among neutral interstellar sight lines is the result of mantling (Sofia, Cardelli & Savage 1994; Barlow 1978) then this linear trend coupled with the correlations in Figure 4 implies that the chemical composition of the small grain population closely resembles that of mantles. Conversely, if the two-line fit is appropriate for the data in Figure 5, this would imply that the small-grain population incorporates a higher Si-to-Fe ratio than mantles, suggesting that the small grains may be silicon rich, which complements the model results of Sofia et al. (2005). A larger number of well-measured interstellar Si and Fe abundances are needed to distinguish between these two interpretations for the small grains.

We gratefully acknowledge partial support from Illinois NASA Space Grant Consortium grant number NGT5-40073 subcontract to Northwestern University, and the Space Telescope Science Institute grant GO-9465.01 to Whitman College.

The authors would like to thank the referee, Dr. Jeffrey Linsky, for his helpful comments that have improved this paper. We would also like to thank David Knauth for his discussions on the material of this paper.

## REFERENCES

- Bahcall, J. N. & Wolf, R. A. 1968, *ApJ*, 152, 701
- Barlow, M. J. 1978, *MNRAS*, 183, 417
- Bergeson, S.D., Mullman, K.L., & Lawler, J. E. 1994, *ApJ*, 435, L159
- Bowen, D. V., Roth, K. C., Meyer, D. M. & Blades, J. C. 2000, *ApJ*, 536, 225
- Calamai, A. G., Smith, P. L., & Bergeson, S. D. 1993, *ApJ*, 451, L59
- Cardelli, J. A., & Savage, B. D. 1995, *ApJ*, 452, 275
- Cardelli, J. A., Sofia, U. J., Savage, B. D., Keenan, F. P., & Dufton, P. L. 1994, *ApJ*, 420, L29
- Cartledge, S. I. B., Meyer, D. M., & Lauroesch, J. T. 2003, *ApJ*, 597, 408
- Cartledge, S. I. B., Lauroesch, J. T., Meyer, D. M., & Sofia, U. J. 2004, *ApJ*, 613, 1037
- Cartledge, S. I. B., Meyer, D. M., Lauroesch, J. T., & Sofia, U. J. 2001, *ApJ*, 562, 394
- Clayton, G. C., Wolff, M. J., Sofia, U. J., Gordon, K. D., & Misselt, K. A. 2003, *ApJ*, 588, 871
- Desert, F. X., Boulanger, F., & Puget, J. L. 1990, *A&A*, 237, 215
- Draine, B. T. 2003, *ARA&A*, 41, 241
- Fitzpatrick, E. L., & Massa, D. 1988, *ApJ*, 328, 734
- . 1997, *ApJ*, 475, 623
- Gull, T. R., Vieira, G., Bruhweiler, F., Nielsen, K. E., Verner, E. & Danks, A. 2005, *ApJ*, 620, 442
- Howk, J. C., Savage, B. D., & Fabian, D. 1999, *ApJ*, 525, 253
- Howk, J. C., Sembach, K. R., Roth, K. C., & Kruk, J. W. 2000, *ApJ*, 544, 867
- Jenkins, E. B. 1987, in *Interstellar Processes*, ed. D. J. Hollanbach & H. A. Thronson (Dordrecht:Reidel), 533
- Jenkins, E. B., Drake, J. F., Morton, D. C., Rogerson, J. B., Spitzer, L., & York, D. G. 1973, *ApJ*, 181, L122

- Jenkins, E. B., Savage, B. D., & Spitzer, L. Jr. 1986, *ApJ*, 301, 355
- Keenan, F. P., Hibbert, A., Burke, P. G., Berrington, K. A. 1988, *ApJ*, 332, 539
- Lagrange, A.-M., Plazy, F., Beust, H., Mouillet, D., Deleuil, M., Ferlet, R., Spyromilio, J., Vidal-Madjar, A., Tobin, W., Hearnshaw, J. B., Clark, M. & Thomas, K. W. 1996, *A&A*, 310, 547
- Larson, K. A., & Whittet, D. C. B. 2005, *ApJ*, 623, 897
- Li, A., & Draine, B. T. 2001, *ApJ*, 550, L213
- Lodders, K. 2003, *ApJ*, 591, 1220
- Mathis, J. S. 1996, *ApJ*, 472, 643
- Mathis, J. S., Rumpl, W., & Nordsieck, K. H. 1977, *ApJ*, 2217, 425
- Morton, D. C. 2003, *ApJS*, 149, 205
- Raassen, A. J. J., & Uylings, P. H. M. 1998, *A&A*, 340, 300
- Savage, B. D., Cardelli, J. A., & Sofia, U. J. 1992, *ApJ*, 401, 706
- Savage, B. D., & Sembach, K. R. 1996, *ApJ*, 470, 893
- Sembach, K., Savage, B. D., & Massa, D. 1991, *ApJ*, 372, 81
- Smeding, A. G. & Pottasch, S. R. 1979, *A&AS*, 35, 257
- Snow, T. P., Rachford, B. L., & Figowski, L. 2002, *ApJ*, 573, 662
- Sofia, U. J., Cardelli, J. A., & Savage, B. D. 1994, *ApJ*, 430, 650
- Sofia, U. J., Gordon, K. D., Clayton, G. C., Misselt, K., Wolff, M. J., Cox, N. L. J., & Ehrenfreund, P. 2006, *ApJ*, 636, 753
- Sofia, U. J., Lauroesch, J. T., Meyer, D. M., & Cartledge, S. I. B. 2004, *ApJ*, 605, 272
- Sofia, U. J., Wolff, M. J., Rachford, B., Gordon, K. D., Clayton, G. C., Cartledge, S. I. B., Martin, P. G., Draine, B. T., Mathis, J. S., Snow, T. P., & Whittet, D. C. B. 2005, *ApJ*, 625, 167
- Spitzer, L. Jr., & Fitzpatrick, E. L. 1993, *ApJ*, 409, 299
- . 1995, *ApJ*, 445, 196

Valencic, L. A., Clayton, G. C., & Gordon, K. D. 2004, *ApJ*, 616, 912

van Steenberg, M. E., & Shull, J. M. 1988 *ApJ*, 330, 942

Vladilo, G. 2002, *ApJ*, 569, 303

Welty, D. E., Hobbs, L. M., Lauroesch, J. T., Morton, D. C., Spitzer, L. Jr., & York, D. G.  
1999, *ApJS*, 124, 465

Zubko, V., Dwek, E., & Arendt, R. G. 2004, *ApJS*, 152, 211

Table 1. Sight Line Characteristics with Iron and Silicon Abundances

| Star               | $E(B - V)^a$<br>(mag) $R_V^b$ $c_4^b$ $N(H)^a$ ( $10^{21} \text{ cm}^{-2}$ ) |     |      |         | Fe II              |                     |                                      |                       | Si II <sup>c</sup>  |   |                       |
|--------------------|--|-----|------|---------|--------------------|---------------------|--------------------------------------|-----------------------|---------------------|---|-----------------------|
|                    |  |     |      |         | Line Listed<br>(Å) | $W_\lambda$<br>(mÅ) | $N$<br>( $10^{14} \text{ cm}^{-2}$ ) | $\delta(\text{Fe})^c$ | $W_\lambda$<br>(mÅ) | $N$<br>( $10^{15} \text{ cm}^{-2}$ ) <sup>d</sup> | $\delta(\text{Si})^c$ |
| HD 27778           | 0.36   | 2.6 | 1.00 | 2.3±0.4 | 2260               | 24.7±0.5            | 2.61±0.05                            | -2.49±0.18            | <2.45 <sup>e</sup>  | <8.62 <sup>e</sup>                                | <-1.04                |
| HD 37021           | 0.54   | 5.8 | 0.04 | 4.8±1.1 | 2367               | 10.4±0.6            | 27.9±1.5                             | -1.78±0.24            | 2.83±0.64           | 14.3±3.2  | -1.14±0.14            |
| HD 37061           | 0.45   | 4.3 | 0.21 | 5.4±1.1 | 2367               | 10.3±0.4            | 27.6±1.0                             | -1.83±0.21            | 2.89±0.36           | 14.4±1.8  | -1.18±0.11            |
| HD 147888          | 0.52   | 3.9 | 0.34 | 5.9±0.9 | 2367               | 8.39±0.52           | 23.1±1.4                             | -1.95±0.16            | 2.58±0.47           | 13.1±2.4  | -1.26±0.37            |
| HD 152590          | 0.39   | ... | ...  | 2.9±0.3 | 2249               | 93.4±2.4            | 15.5±0.4                             | -1.81±0.11            | 1.68±0.55           | 8.31±2.71   | -1.15±0.048           |
| HD 207198          | 0.59   | 2.8 | 0.77 | 4.8±1.1 | 2249               | 78.8±1.2            | 13.5±2.1                             | -2.09±0.28            | 1.40±0.68           | 6.91±3.35   | -1.45±0.26            |
| ζ Oph <sup>f</sup> | 0.60   | 2.6 | 0.56 | 1.4±0.1 | 2249               | 22.5±1.1            | 3.09±.14                             | -2.20±0.09            | 0.48±0.12           | 2.89±0.68   | -1.30±0.34            |

<sup>a</sup>Cartledge et al. (2004).

<sup>b</sup>Valencic, Clayton, & Gordon (2004).

<sup>c</sup>Inferred logarithmic depletions of Fe and Si into the dust-phase based upon the derived column densities, the total hydrogen column densities listed, and the the proto-solar abundance value for Fe and Si from Lodders (2003). Si II columns derived from the 2335Åline.

<sup>d</sup>Errors listed include continuum placement and photon noise errors only, errors including the uncertainty in oscillator strength are (in units of  $10^{15} \text{ cm}^{-2}$ ) 4.1, 3.2,3.4, 3.10, 3.58, and 0.89 for the six detections respectively.

<sup>e</sup>3  $\sigma$  limit.

<sup>f</sup>The Fe II  $W_\lambda$  is from Savage, Cardelli & Sofia (1992). Savage, Cardelli & Sofia (1992) used now outdated  $f$ -values in their determination of the Fe II column density towards ζ Oph. This value has been changed to reflect the current  $f$ -value for the 2249 Å transition (Howk et al. 2000). The Si II  $W_\lambda$  is from Cardelli et al. (1994). ζ Oph has two absorbing components, but Cardelli et al. (1994) could only measure the 2335 Å transition for the stronger component B. Sofia, Cardelli & Savage (1994) report the column density for component A, based on measurements of Si II  $\lambda$ 1808 (Savage, Cardelli & Sofia 1992), and component B. The two components have been combined here.

Table 2. EQWs and Optically–thin Column Densities for HD 147888

| Fe II line<br>(Å) | $\log(\lambda f)$ | $W_\lambda$<br>(mÅ) | $N$<br>(cm <sup>-2</sup> )      |
|-------------------|-------------------|---------------------|---------------------------------|
| 1055              | 0.81              | 28.2±3.8            | (5.43±0.74) × 10 <sup>14</sup>  |
| 1142              | 0.66              | 42.2±9.9            | (1.06±0.25) × 10 <sup>15</sup>  |
| 1143              | 1.34              | 38.9±5.3            | (2.22±0.30) × 10 <sup>14</sup>  |
| 1144              | 1.98              | 105±5               | (1.40±0.06) × 10 <sup>14</sup>  |
| 2234              | -1.54             | 1.20±0.3            | (1.10±0.25) × 10 <sup>15</sup>  |
| 2249              | 0.61              | 44.2±0.8            | (1.06±0.02) × 10 <sup>15</sup>  |
| 2260              | 0.74              | 59.3±0.8            | (9.87±0.13) × 10 <sup>14</sup>  |
| 2367              | -0.71             | 8.39±0.52           | 2.31±0.14 × 10 <sup>15</sup>    |
| 2344              | 2.43              | 227±1               | (1.41±0.004) × 10 <sup>14</sup> |
| 2374              | 1.87              | 163±1               | (2.80±0.01) × 10 <sup>14</sup>  |
| 2382              | 2.88              | 266±1               | (7.38±0.03) × 10 <sup>13</sup>  |

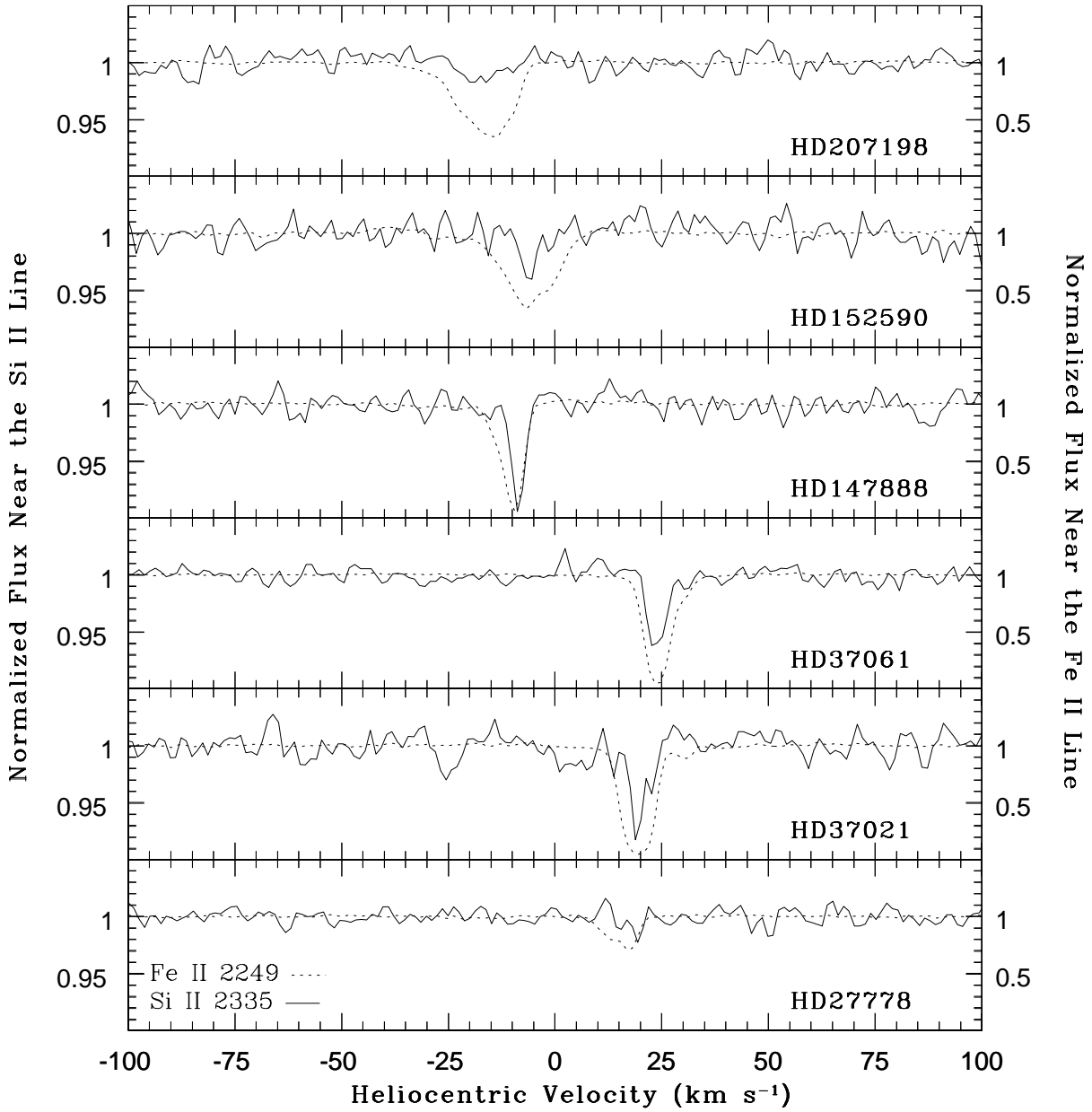


Fig. 1.— Normalized STIS echelle spectra of the Si II]  $\lambda 2335$  (solid line) and Fe II  $\lambda 2249$  (dotted line) absorption features. Note that the normalized flux scale is on the left for silicon and on the right for iron.



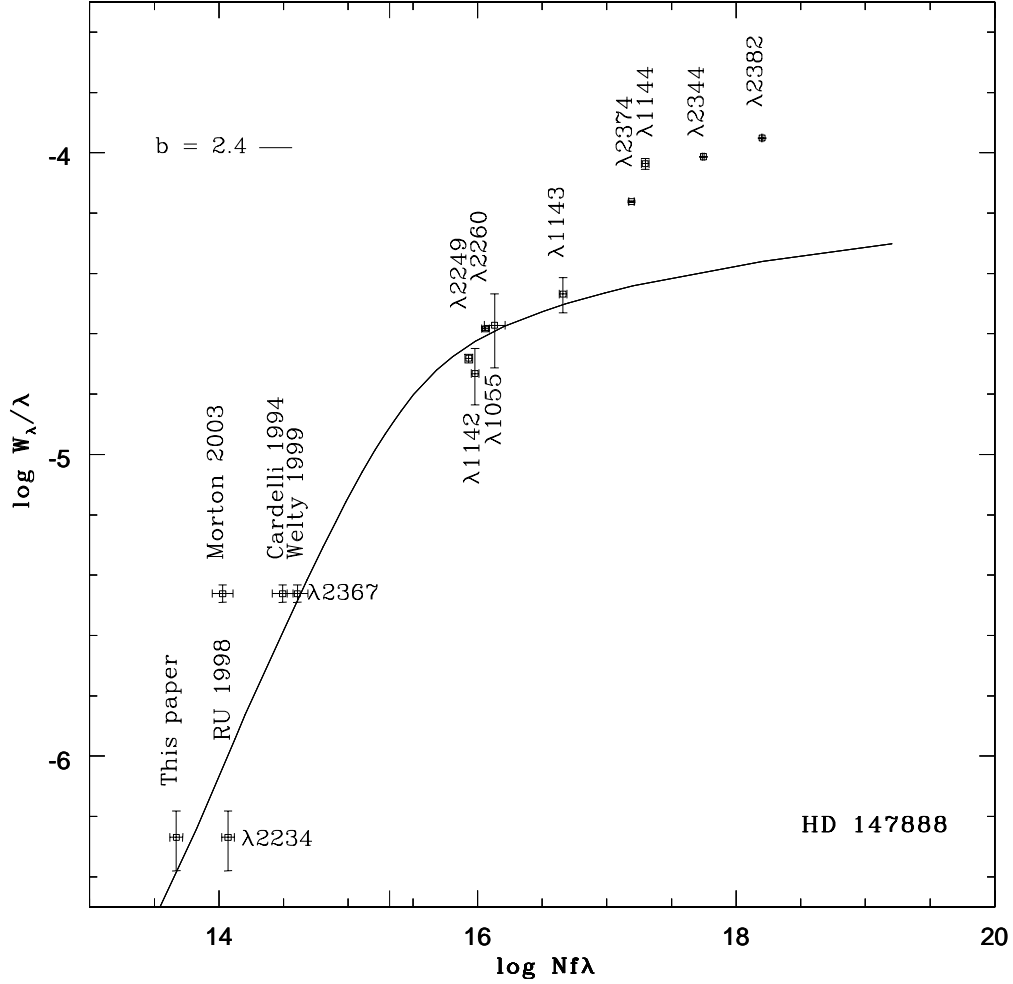


Fig. 2.— Curve of growth for Fe II absorption lines toward HD 147888, based on *STIS* and *FUSE* data. The lines at  $\lambda$  1144, 2344, 2374, 2382 Å have appear to have larger equivalent widths than would be expected based on the low  $f$ -value lines, because there are a few low column density components along this sight line that are not measurably represented in the weaker lines. These low column density components are outside the main component(s) seen in Figure 1 (with a best fit doppler width  $b = 2.4 \text{ km s}^{-1}$ ), but do provide a significant addition to the equivalent widths of the stronger lines, and therefore these lines fail to follow the curve of growth. These components are however, justifiably ignored for the purposes of this analysis due to their low total column and lack of corresponding Si II] 2335 Å absorption. The three different oscillator strengths for Fe II 2367 Å are shown, showing that the Welty et al. (1999) value is the best choice. Both oscillator strengths for Fe II 2234Å, the one calculated by Raasen & Uylings (1998) and the one determined in this paper, are shown. The  $f$ -value calculated by Raasen & Uylings (1998) appears to underestimate the total Fe II column density. Uncertainties in the oscillator strengths are shown by the horizontal error bars (see text).

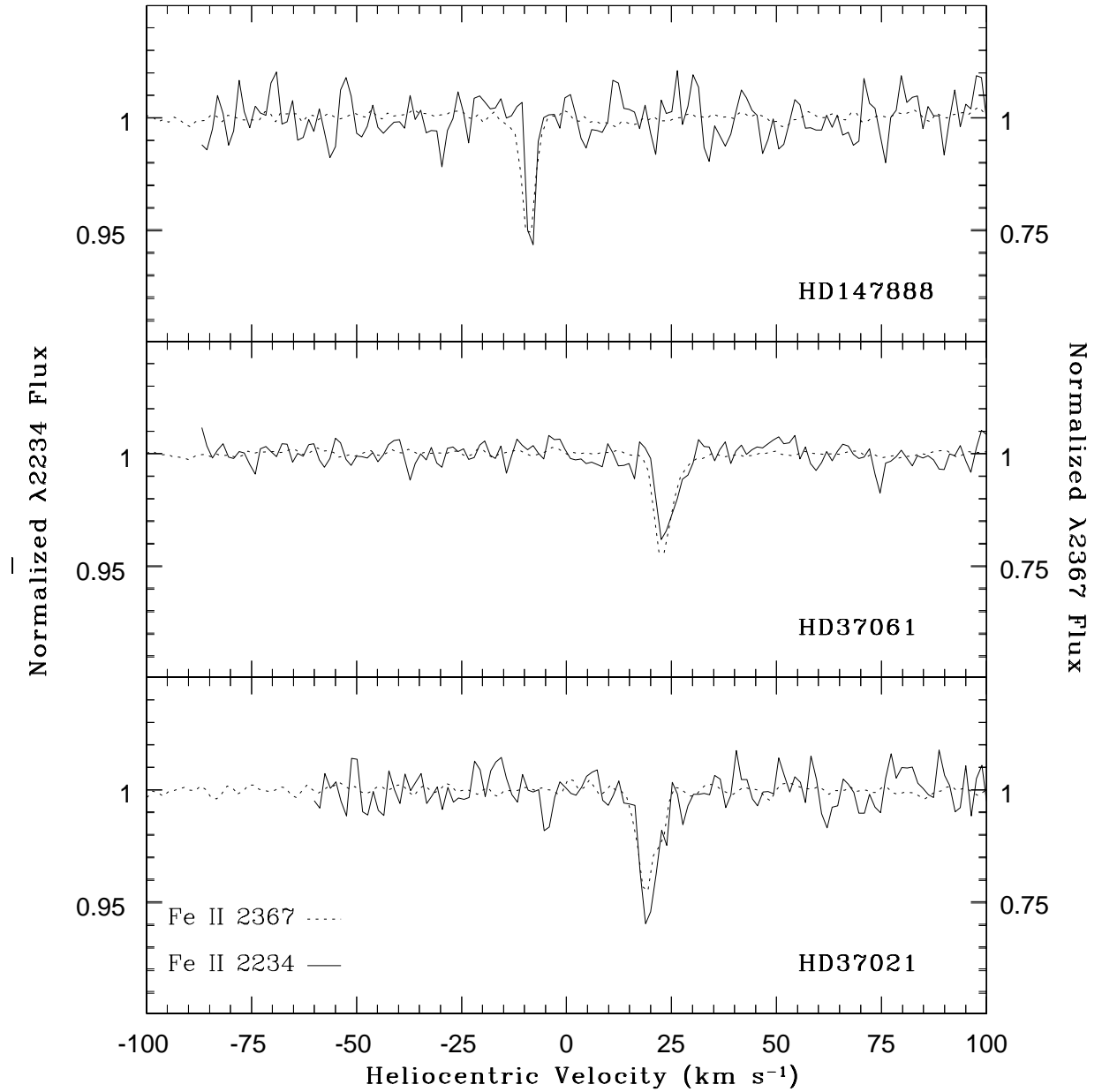


Fig. 3.— Normalized STIS echelle spectra of the Fe II  $\lambda 2234$  (*solid line*) and Fe II  $\lambda 2367$  (*dotted line*) absorption features. Note that the normalized flux scale is on the left for the 2234 Å and on the right for the 2367 Å data.

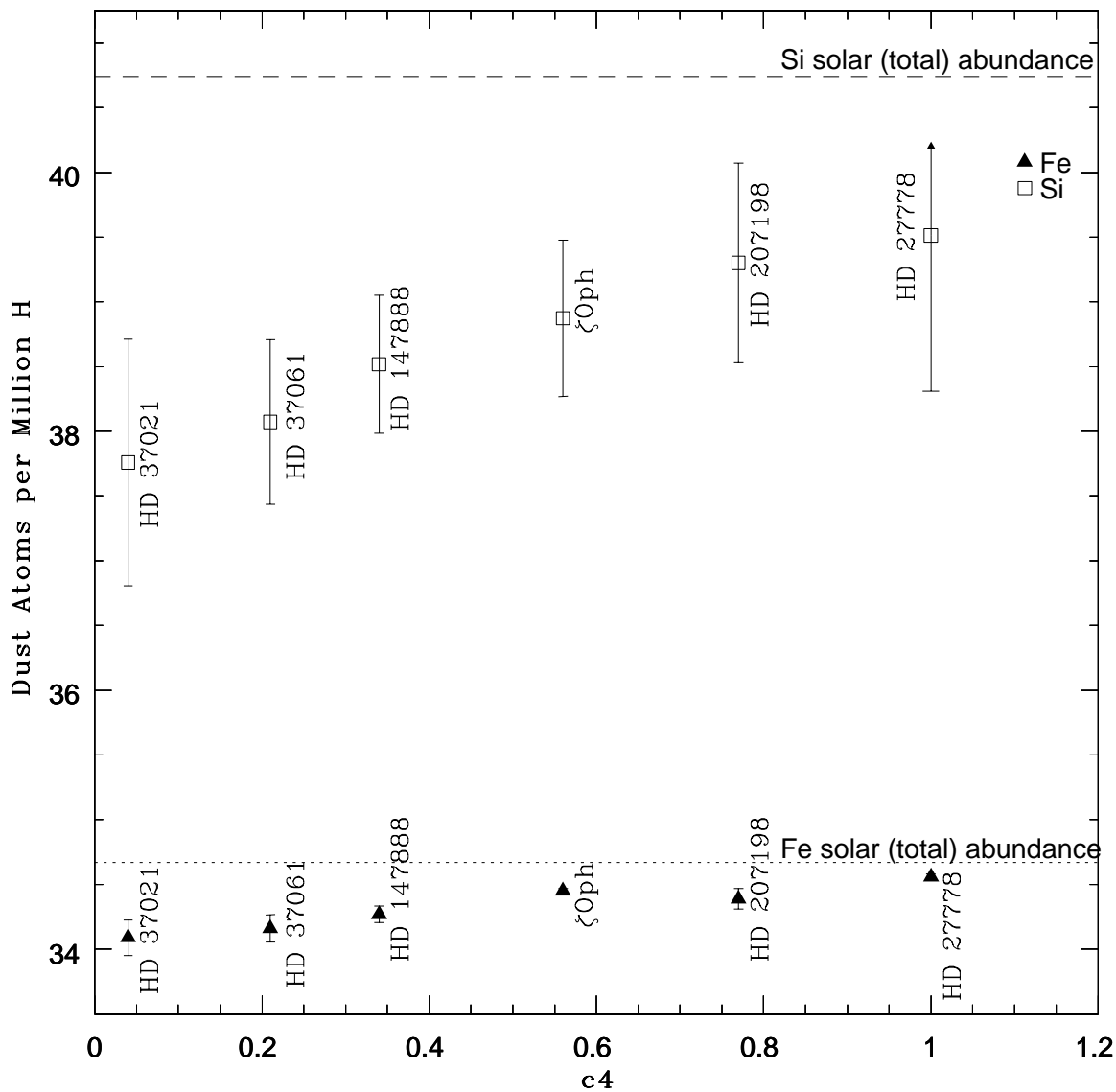


Fig. 4.— Number of silicon and iron atoms in the dust per  $10^6$  H versus the Fitzpatrick & Massa (1988) extinction coefficient  $c_4$ , with  $1 \sigma$  error bars. The  $c_4$  parameter describes the strength of the rise toward the far-ultraviolet, and is believed to be related to the abundance of small grains. Note that the iron uncertainties for  $\zeta$  Oph and HD 27778 are less than the size of the point on the plot. The proto-solar abundance values are from Lodders (2003).

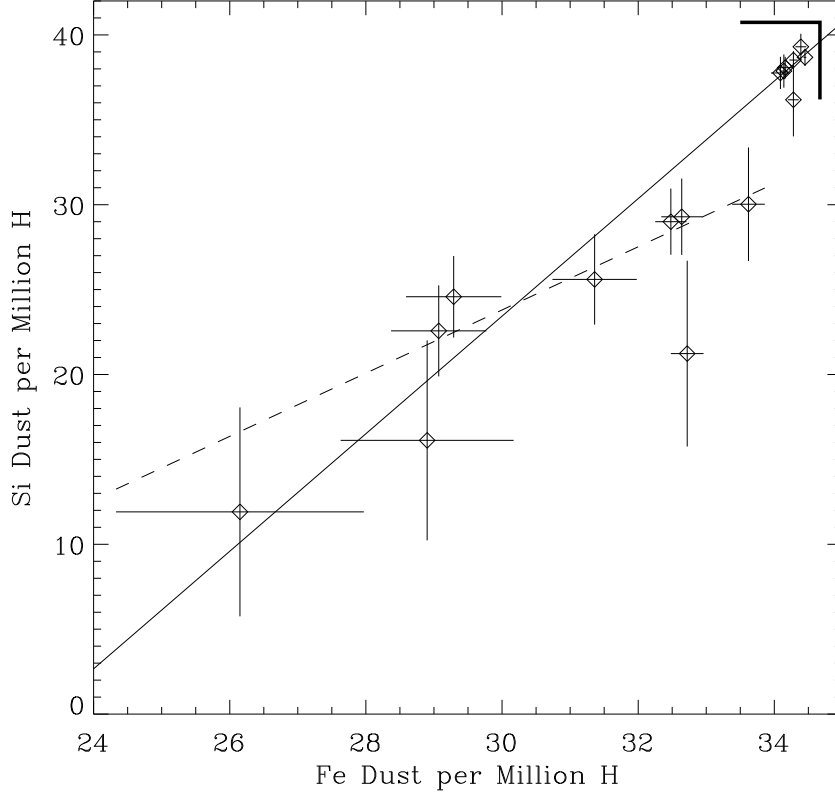


Fig. 5.— Dust-phase Si nuclei per million H nuclei versus dust-phase Fe nuclei per million H nuclei, with  $1\sigma$  error bars. The sight line (component, if necessary) - and source for each point on this plot from left to right are: HD 149881(2) - Spitzer & Fitzpatrick (1995), HD 93521(3) - Spitzer & Fitzpatrick (1993), HD 93521(6), HD 149881(6), HD 18100 - Savage & Sembach (1996), HD 215733(19) - Fitzpatrick & Spitzer (1997), HD 93521(8),  $\mu$  Col(1) - Howk, Savage & Fabian (1999), 23 Ori(WLV) - Welty et al. (1999), and the 7 points in the upper right hand portion of the plot are the sight lines from Table 1, minus HD 27778, and 23 Ori(SLV) (Welty et al. 1999) which lies below the others. Note that HD 27778 is not included in this plot as only an upper limit is available for Si. The solar abundance values for Si and Fe (Lodders 2003) are shown by the bold lines in the upper right hand portion of the plot. The solid line is a least squares fit to all the data shown, while the dashed line represents a fit to only those points with less than 34 iron atoms in the dust per million H atoms.